

CRONIN EFFECT IN PROTON-NUCLEUS COLLISIONS: A SURVEY OF THEORETICAL MODELS*

A. Accardi

Institut für Theoretische Physik der Universität Heidelberg,
Philosophenweg 19, D-69120 Heidelberg, Germany.
e-mail: accardi@tphys.uni-heidelberg.de

Abstract

I compare the available theoretical models that describe the Cronin effect on hadron and minijet production in proton-nucleus collisions, pointing out similarities and differences among them. The effect may be summarized by the value of two variables. Their values computed in the different models are compared in the energy range 27.4 GeV - 5500 GeV. Finally, I propose to use the pseudorapidity systematics as a further handle to distinguish among the models.

1 INTRODUCTION

In this short note I will compare available theoretical models for the description of the so-called Cronin effect [2] in inclusive hadron spectra in proton-nucleus (pA) collisions. The analysis will be limited to references containing quantitative predictions in the case of pA collisions [3–7]. The observable which I am interested in is the *Cronin ratio*, R , of the inclusive differential cross-sections for proton scattering on two different targets, normalized to the respective atomic numbers A and B :

$$R(p_T) = \frac{B}{A} \frac{d\sigma_{pA}/d^2p_T}{d\sigma_{pB}/d^2p_T} .$$

In absence of nuclear effects one would expect $R(p_T)=1$, but for $A>B$ a suppression is observed experimentally at small p_T , and an enhancement at moderate p_T with $R(p_T) \rightarrow 1$ as $p_T \rightarrow \infty$. This behaviour may be characterized by the value of three parameters: the transverse momentum p_\times at which R crosses unity and the transverse momentum p_M at which R reaches its maximum value $R_M=R(p_M)$, see Fig. 1. These *Cronin parameters* will be studied in Sec. 3

The Cronin effect has received renewed interest after the experimental discovery at RHIC of an unexpectedly small $R < 1$ in Au-Au collisions at $\sqrt{s}=130$ GeV compared to pp collisions at the same energy [8]. This fact has been proposed as an experimental signature of a large jet quenching suggesting that a Quark-Gluon Plasma was created during the collision [9]. However, the extrapolation to RHIC and LHC energies of the known Cronin effect at lower energies is haunted by large theoretical uncertainties, which may make unreliable any interpretation of signals of this kind. Some light will be shed on this problem by the upcoming RHIC data on dA collisions at $\sqrt{s}=200$ GeV.

Since in pA collisions no hot and dense medium is expected to be created, a pA run at the same nucleon-nucleon energy as in nucleus-nucleus (AA) collisions would be of major importance to test the theoretical models and to have reliable baseline spectra for the extraction of novel physical effects. A further advantage of pA collisions, is that the multiplicity of particles in the final state is relatively small compared to AA collisions. For this reason at ALICE minijets may be observed at transverse momenta larger than 5 GeV (see Section on “The experimental parameters for pA at the LHC” in Ref. [1]). As I will discuss in Sec. 3, this may allow the use of the Cronin effect on minijet production as a further check of the models.

*Contribution to the CERN Yellow report on Hard Probes in Heavy Ion Collisions at the LHC.

2 THE MODELS

Soon after the discovery of the Cronin effect [2], it was realized that the observed nuclear enhancement of the p_t -spectra could be explained in terms of multiple interactions [10, 11]. The models may be classified according to the physical object which is undergoing rescatterings (the projectile hadron or its partons), and to the ‘‘hardness’’ of the rescattering processes taken into account. Note that a parton is commonly said to undergo a hard scattering if the exchanged momentum is of the order or greater than approximately 1 GeV. However, physically there is no sharp distinction between soft and hard momentum transfer. Therefore, I prefer to make reference to the so-called two component models of hadron transverse spectra, and call hard a scattering which is described by a power-law differential cross-section at large p_t , and soft a scattering whose cross-section is decreasing faster than any inverse power of the transverse momentum at large p_t . In Tables 2.1 and 2.2 I provide a quick comparison of the hadronic and partonic rescattering models, respectively.

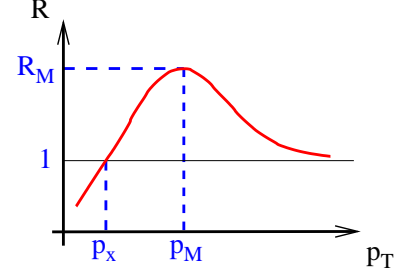


Fig. 1: Definition of p_x , p_M , R_M .

2.1 Soft hadronic rescattering models [3] [4]

These models are based on the pQCD collinearly factorized cross-section for inclusive particle production in pp collisions. In order to describe the large- p_T tail of transverse momentum spectra, one has to include also an intrinsic transverse momentum for the colliding parton. The collision of a proton on a nuclear target of atomic number A is then obtained in a Glauber-type model as follows¹:

$$\frac{d\sigma_{pA}^h}{d^2p_T} = K \sum_{i,j,k,l} F_{i/p} \otimes F_{j/A} \otimes \frac{d\hat{\sigma}}{d\hat{t}}(ij \rightarrow kl) \otimes D_k^h, \quad (1)$$

where the proton and nucleus parton distribution functions are, respectively,

$$F_{i/p} = f_{i/p}(x_i, Q^2) \frac{e^{-k_{iT}^2 / \langle k_T^2 \rangle_p(b)}}{\pi \langle k_T^2 \rangle_{pA}} \quad \text{and} \quad F_{j/A} = T_A(b) f_{j/p}(x_j, Q^2) \frac{e^{-k_{jT}^2 / \langle k_T^2 \rangle_{Ap}(b)}}{\pi \langle k_T^2 \rangle_A}. \quad (2)$$

In Eq. (1) $d\hat{\sigma}/d\hat{t}(ij \rightarrow kl)$ is the pQCD parton-parton cross-section, the variables with a hat are the Mandelstam variables at parton level, and a sum over incoming and outgoing parton flavours is performed. The proton is considered point-like compared to the target nucleus, and to scatter on it at impact parameter b . The nucleus is described by the Woods-Saxon nuclear thickness function $T_A(b)$. In Eq. (2) $f_{i/p(A)}(x, Q^2)$ are the parton distribution functions of the proton (nucleus); isospin imbalance is taken into account and nuclear shadowing is included by the HIJING parametrization [12]. Partons are assumed to have an intrinsic transverse momentum with average squared value $\langle k_T^2 \rangle_{pA(Ap)}$ and a Gaussian distribution. Due to the k_i and k_j integrations a regulator mass $m=0.8$ GeV has been used in the pQCD cross-section. Finally, $D_k^h(z, Q^2)$ are the fragmentation functions of a parton k into a hadron h with a fraction z of the parton momentum.

Soft proton-nucleon interactions are assumed to excite the projectile proton’s wavefunction, so that when the proton interacts with the next target nucleon its partons have a broadened intrinsic momentum. Each rescattering of the proton is assumed to contribute to the intrinsic momentum broadening in the same way, so that:

$$\langle k_T^2 \rangle_{pA}(b, \sqrt{s}) = \langle k_T^2 \rangle_{pp} + \delta \times h_A(b, \sqrt{s}), \quad (3)$$

¹Integrations are schematically indicated with crossed circle symbols. For details see the original references.

Table 2.1 – Parameters of the soft hadronic rescattering models. [4].

model	hard scales GeV	K	regul.	proton intrinsic k_T (GeV ²)	n	average k_T -kick (GeV ²)	nPDF
Soft	$Q = Q' = p_T$	2	0.8 GeV	$\langle k_T^2 \rangle_{pp} = 1.2 + 0.2\alpha_s(q^2)q^2$ [†]	∞	$\delta(Q) = 0.255 \frac{\ln^2(Q/\text{GeV})}{1 + \ln(Q/\text{GeV})}$	HIJING
Soft-sat.	$Q = \frac{p_T}{2z_c}$; $Q' = \frac{p_T}{2}$ ^b	1	0.8 GeV	$\langle k_T^2 \rangle_{pp} = F(\sqrt{s})$ [‡]	4	$\delta = 0.4$	HIJING

[†] $q^2 = 2\hat{s}\hat{t}\hat{u}/(\hat{s} + \hat{t} + \hat{u})^2$; parametrization chosen to best reproduce pp data.

[‡] No explicit parametrization is given. Values of $\langle k_T^2 \rangle_{pp}$ extracted from a “best fit” to pp data, see Fig.15 of Ref. [4].

^b These scales used in the computations of Table 3. In Ref. [4] $Q = \frac{p_T}{2}$ and $Q' = \frac{p_T}{2z_c}$.

where $\langle k_T^2 \rangle_{pp}$ is the proton intrinsic momentum needed to describe hadron transverse spectra in pp collisions, δ is the average momentum squared acquired in each rescattering, and

$$h_A(b, \sqrt{s}) = \begin{cases} \nu_A(b, \sqrt{s}) - 1 & \text{if } \nu_A - 1 \leq n \\ n & \text{if } \nu_A - 1 > n \end{cases} \quad (4)$$

represent the average number of collisions which are effective in broadening the intrinsic momentum. Both models assume h_A to be a function of the number of proton-nucleon collisions $\nu_a(b, \sqrt{s}) = \sigma_{pp}(\sqrt{s})T_A(b)$, with σ_{pp} the nucleon-nucleon inelastic cross-section. However, Ref. [3] takes $m=\infty$, while Ref. [4] assumes an upper limit $n=4$ justified in terms of a proton dissociation mechanism: after a given number of interactions the proton is so excited that it can no more interact as a whole with the next nucleon. I will call the first model simply *soft* and the second *soft-saturated*. In both models target nucleon do not have rescatterings, so that

$$\langle k_T^2 \rangle_{Ap}(b, \sqrt{s}) = \langle k_T^2 \rangle_{pp}$$

Further differences between the models are related to the choices of the hard-scales, of the K -factor which simulates NLO contributions to the parton cross-section, and to the parametrizations of $\langle k_T^2 \rangle_{pp}$ and δ (see Table 2.1).

2.2 Soft partonic rescatterings: the colour dipole model [5]

In this model the particle production mechanism is controlled by the *coherence length* $l_c = \sqrt{s}/(m_N k_T)$, where m_N is the nucleon mass and k_T the transverse momentum of the parton which fragments in the observed hadron. Depending on the value of l_c , three different calculational schemes are considered. (a) In fixed target experiments at low energy (e.g., at SPS), where $l_c \ll R_A$, the projectile’s partons interact incoherently with target nucleons and high- p_t hadrons are assumed to originate mainly from projectile’s parton which underwent a hard interaction and whose transverse momentum was broadened by soft parton rescatterings. The parton is then put on-shell by a single semihard scattering computed in factorized pQCD. This scheme I will discuss in detail below. (b) At LHC, where the c.m. energy is very large and $l_c \gg R_A$, the partons interact coherently with the target nucleons and high- p_T hadrons are assumed to originate from radiated gluons; parton scatterings and gluon radiation are computed in the light-cone dipole formalism in the target rest frame. (c) At intermediate energies, like at RHIC, an interpolation is made between the results of the low- and high- energies regimes discussed above. All the phenomenological parameters needed in this model are fixed in reactions different from pA collisions, and in this sense the model is said to be parameter-free.

In the short coherence length scheme, pQCD factorization is assumed to be valid and formula (1) is used with parton masses $m_g=0.8$ GeV and $m_q=0.2$ GeV for, viz., gluons and quarks. Moreover,

$$F_{i/p} = f_{i/p}(x_i + \frac{\Delta E}{x_a E_p}, Q^2) \frac{dN_i}{d^2 k_{iT}}(x, b) \quad \text{and} \quad F_{j/A} = T_A(b) f_{j/p}(x_j, Q^2) \frac{dN_j^{(0)}}{d^2 k_{jT}}(x, b).$$

Table 2.2 – Parameters of the soft partonic rescattering model (at short- l_c) and of the hard partonic rescattering models.

model	hard scales	K	regulators (GeV)	intr. k_T	dE/dz	dipole cross-sect.	nPDF
Col. dip.	$Q = Q' = p_T$	\otimes	$m_g=0.8, m_q=0.2$	as Soft mod.	-2.5 GeV/fm	$\sigma_0=23$ mb, $\lambda=0.288, x_0=3 \cdot 10^{-4}$	EKS98 [†]
Hard AT	$Q = Q' = p_T^*$	2	μ free param.	no	no	computed from pQCD	no
Hard GV	$Q = Q' = p_T$	\otimes	$\mu=0.42^b$	as Soft mod.	no	—	EKS98

* $Q=\mu$ in Ref. [6]. [†] Only at large x_j (EMC effect). \otimes Factors out in the Cronin ratio.

^b μ determines only the typical momentum transfer in elastic rescatterings.

Parton rescatterings are computed in terms of the propagation of a $q\bar{q}$ pair through the target nucleus, and the final parton transverse momentum distribution dN_i/d^2k_{iT} is written as:

$$\frac{dN_i}{d^2k_{iT}} = \int d^2r_1 d^2r_2 e^{i\vec{k}_T \cdot (\vec{r}_1 - \vec{r}_2)} \left[\frac{\langle k_0^2 \rangle}{\pi} e^{-\frac{1}{2}(r_1^2 + r_2^2) \langle k_0^2 \rangle} \right] \left[e^{-\frac{1}{2} \sigma_{q\bar{q}}^N(\vec{r}_1 - \vec{r}_2, x) T_A(b)} \right] = \frac{dN^{(0)}}{d^2k_T} + O(\sigma_{q\bar{q}}^N T_A). \quad (5)$$

The first bracket in Eq. (5) represents the contribution of the proton intrinsic momentum. The second bracket is the contribution of soft parton rescatterings on target nucleons, expressed through the phenomenological dipole cross-section: for a quark, $\sigma_{q\bar{q}}^N(r_T, x) = \sigma_0 [1 - \exp(-\frac{1}{4} r_T^2 Q_s^2(x))]$ with $Q_s=1 \text{ GeV}(x/x_0)^{\lambda/2}$ (for the value of the parameters see Table 2.2); for a gluon $\sigma_{g\bar{g}}^N=9/4 \sigma_{q\bar{q}}^N$ is used. The expansion of Eq. (5) to zeroth order in $\sigma_{q\bar{q}}^N$ gives the intrinsic k_T distribution $dN^{(0)}/d^2k_T$ of the nucleon partons; the first order term represents the contribution of one-rescattering processes, and so on. Partons from the target nucleus are assumed not to undergo rescatterings because of the small size of the projectile. Energy loss of the projectile partons is taken into account by a shift of their fractional momentum proportional to the energy of the radiated gluons, given by the product of the average mean path length ΔL and the energy loss rate dE/dz [15]. As nuclear shadowing effects are computed theoretically in the dipole formalism, see Eq. (5), parton distribution functions in the target are modified only to take into account antishadowing at large x according to the EKS98 parametrization [14].

By Fourier transforming the dipole cross-section one sees that the transverse momentum distribution of the single parton-nucleon scattering is Gaussian, whence the classification of this model among the “soft” ones. However, the single distributions are not just convoluted obtaining a broadening proportional to the average number of rescatterings. Indeed, in the second bracket the rescattering processes have a Poisson probability distribution. As a result, the nuclear broadening of the intrinsic momentum is smaller than the product of the average number of rescatterings and the single scattering broadening; this might give a dynamical explanation of the assumption used in the Soft-saturated model [4], that $n \not\ll \infty$ in Eq. (4).

2.3 Hard partonic rescattering model [6] [7]

The model of Ref. [6], hereafter labeled “hard AT”, assumes parton rescatterings responsible of the Cronin enhancement, and includes up to now in the computations only semihard scatterings, i.e., scatterings described by the pQCD parton-parton cross-section. It is the generalization to an arbitrary number of hard parton rescatterings of the early models of Refs. [10, 11, 16] and of the more recent Refs. [17, 18], limited to 1 hard rescattering. As shown in Ref. [11], considering only one rescattering may be a reasonable assumption at low energy to describe the gross features of the Cronin effect, but already at RHIC energies this might not be enough for the computation of the Cronin peak R_M [6]. The AT model assumes the S-matrix for a collision of n partons from the on m partons from the target to be factorizable in terms of S-matrices for parton-parton elastic-scattering, and assumes generalized pQCD factorization

[19]. The result is a unitarized cross-section, as discussed in Refs. [6, 20]:

$$\frac{d\sigma_{pA}^h}{d^2p_T} = \sum_i f_{i|p} \otimes \frac{dN_{i|A}}{d^2k_T} \otimes D_i^h + \sum_j f_{j|A} T_A \otimes \frac{dN_{j|p}}{d^2k_T} \otimes D_j^h. \quad (6)$$

The first term accounts for multiple semihard scatterings of proton partons on the nucleus; in the second term the nucleus partons are assumed to undergo a single scattering, and $\frac{dN_{j|p}}{d^2k_T} = \sum_i f_{i|p} \otimes \sigma_{i|H}^N$. Nuclear effects are included in dN_i^H/d^2k_T , the average transverse momentum distribution of a proton parton who suffered *at least* one semihard scattering. In impact parameter space it reads

$$\frac{dN_{i|A}}{d^2k_T}(b) = \int \frac{d^2r}{4\pi} e^{-i\vec{k}_T \cdot \vec{r}} \left[e^{-\sigma_{i|H}^N(r)T_A(b)} - e^{-\sigma_{i|H}^N T_A(b)} \right], \quad (7)$$

where unitarity is explicitly implemented at the nuclear level, as discussed in Ref. [20]. In Eq. (7) $\sigma_{i|H}^N(r) = K \sum_j \int d^2p [1 - e^{-i\vec{p} \cdot \vec{r}}] \frac{d\hat{\sigma}}{dt}(ij \rightarrow ij) \otimes f_{j|p}$. Moreover, $\omega_i \equiv \sigma_{i|H}^N T_A(b)$ (i.e., the parton-nucleon semihard cross-section times the thickness function) is identified with the target opacity to the parton propagation. Note that $\sigma_{i|H}^N(r) \propto r^2$ as $r \rightarrow 0$ and $\sigma_{i|H}^N(r) \rightarrow \sigma_{i|H}^N$ as $r \rightarrow \infty$. This, together with the similarity of Eqs. (7) and (5) suggests the interpretation of $\sigma_{i|H}^N(r)$ as a *hard dipole cross-section*, which accounts for hard parton rescatterings analogously to what $\sigma_{q\bar{q}}^N$ does for soft parton rescatterings. Note that no nuclear effects on PDF's are included, but shadowing is partly taken into account by the multiple scattering processes.

To regularize the IR divergences of the pQCD cross-sections a small mass regulator μ is introduced in the parton propagators, and is considered a free parameter of the model which signals the scale at which pQCD computations break down. As a consequence of the unitarization of the interaction, due to the inclusion of rescatterings, both p_\times and p_M are almost insensitive on μ [6]. For this reason these two quantities are considered a reliable prediction of the model². Note, however, that they both depend on the c.m. energy \sqrt{s} and on the pseudorapidity η . On the other hand, R_M is strongly sensitive to the IR regulator. This sensitivity may be traced back to the inverse-power dependence on μ of the target opacity ω_i : $\omega_i \propto 1/\mu^a$, where the power $a > 2$ is energy and rapidity dependent. The divergence of ω_i as $\mu \rightarrow 0$ indicates the need of unitarization of the parton-nucleon cross-section, and deserves further study. Therefore, μ can be here considered only an effective scale which simulates non-perturbative physics not considered here [26, 29], the non-linear evolution of parton distribution functions in the target [30] and physical effects up to now neglected, e.g., collisional and radiative energy losses [31].

In the model of Ref. [7], hereafter labeled “hard GV”, the transverse momentum broadening of a parton which undergoes semihard rescatterings is evaluated with the help of Eq. (7) to be

$$\langle k_T^2 \rangle_H = \omega \mu^2 \ln \left(1 + c \frac{p_T^2}{\mu^2} \right), \quad (8)$$

where the IR regulator μ is physically identified with the medium screening mass and fixed to $\mu = 0.42$ GeV, and represents the typical momentum kick in each elastic rescattering of a hard parton. The factor c and the constant term 1 are introduced in order to obtain no broadening for $p_T \approx 0$ partons, as required by kinematic considerations. The average value in the transverse plane of the opacity $\omega \approx (0.4/\text{fm})R_A$ (with R_A the nuclear radius) and of the factor $c/\mu^2 = 0.18$ are fixed in order to reproduce the experimental data at $\sqrt{s}=27.4$ GeV and $\sqrt{s}=38.8$ GeV [22]. With these values the logarithmic enhancement in Eq. (8) is of order 1 for $p_T \approx 3$ GeV. Note that ω and c are assumed to be independent of \sqrt{s} and η . Finally, the transverse spectrum is computed by using Eq. (1) and adding to the semihard broadening of Eq. (8) the intrinsic momentum of the projectile partons, $\langle k_0^2 \rangle = 1.8$ GeV²:

$$\langle k_T^2 \rangle_{pA} = \langle k_T^2 \rangle_{pp} + \langle k_T^2 \rangle_H,$$

with shadowing and antishadowing corrections to target partons as in the EKS98 parametrization [14].

²This result is very different from the conclusion of Ref. [18], based on a single-rescattering approximation, that $p_\times \propto p_0$. Hence p_\times cannot be used to “measure” the onset of hard dynamics as proposed in that paper.

Table 3 – Cronin effect at $\eta=0$: comparison of theoretical models. p_M is expressed in GeV.

\sqrt{s}	model	charged pions			partons		
		p_M	R_M	Ref.	p_M	R_M	Ref.
27.4 GeV pW/pBe data: Ref. [22]	Soft	4.0	1.55*	[3]	$6 \pm 0.8^\dagger$	$1.1^b; 1.4^b$	[24]
	Soft-saturated	4.5*; 4.4 $^\circ$	1.46*; 1.46 $^\circ$	[24]			
	Color dipole	4.5	1.43 $\pm 0.08^\otimes$	[5]			
	Hard AT						
	Hard GV	4	1.4	[7]			
200 GeV pAu/pp	Soft	3.5	1.35 $\pm 0.2^\ddagger$	[3]	$7 \pm 1^\dagger$	$1.25^b; 1.2^b$	[24]
	Soft-saturated	2.9*; 2.7 $^\circ$	1.15*; 1.47 $^\circ$	[24]			
	Color dipole	2.7	1.1	[5]			
	Hard AT						
	Hard GV	3.0	1.3	[7]			
5500 GeV pPb/pp	Soft	3.5	1.08 $\pm 0.02^\ddagger$	[25]	$11 \pm 1.3^\dagger$	$2.1^b; 1.2^b$	[24]
	Soft-saturated	2.4*; 2.2 $^\circ$	0.78*; 1.36 $^\circ$	[24]			
	Color dipole	2.5	1.06	[5]			
	Hard AT						
	Hard GV	$\approx 40^\diamond$	1.05 $^\diamond$	[7]			

* With HIJING shadowing [12]. $^\circ$ Without shadowing. $^\otimes$ Error estimated by varying dE/dz within error bars [23].

‡ Central value with multiple scattering effects only; error estimated by using different shadowing parametrizations.

† Numerical errors mainly. b Using $\mu = 1.5$ GeV. a Using $\mu = 0.060 + 0.283 \log(\sqrt{s})$, see text.

$^\diamond$ Completely dominated by EKS98 shadowing and anti-shadowing; result considered not reliable as yet, see text.

3 PREDICTIONS AND CONCLUSIONS

In Table 3 I listed the values of the Cronin parameters p_M and R_M computed in the various models for proton-nucleon center-of-mass energy of 27.4 GeV (representing the low-energy experiments at CERN ISR and SPS and at Fermilab), of 200 GeV (RHIC) and of 5500 GeV (LHC). The targets considered in the Cronin ratio are listed as well. Since p_\times is of the order of 1 GeV in almost all models at all energies, and lies at the border of the validity range of the models, it's value is not shown. Uncertainties of the model calculations are included when discussed in the original references (see the notes at the foot of the table). In the case of the soft-saturated model, the uncertainty due to the choice of shadowing parametrization is illustrated by giving the results obtained with no shadowing, beside the results obtained with the HIJING parametrization [12]. Using the “new” HIJING parametrization [13] would change mid-rapidity results only at LHC energy, where a 15% smaller Cronin peak would be predicted [24]³. In the case of the “hard AT” rescattering model, the major theoretical uncertainty lies in the choice of the effective parameter μ as discussed at the end of Sec. 2.3. In the table, two choices are presented: (a) an energy-independent value $\mu = 1.5$ GeV, which leads to an increasing Cronin effect as energy increases; (b) μ is identified with the IR cutoff p_0 discussed in [32], in the context of a leading order pQCD analysis of pp collisions. That analysis found p_0 to be an increasing function of \sqrt{s} . By performing a simple logarithmic fit to the values extracted from data in Ref. [32] we find $\mu = p_0(\sqrt{s}) = 0.060 + 0.283 \log(\sqrt{s})$, leading to a decreasing Cronin effect. Note that a scale increasing with \sqrt{s} appears naturally also in the so-called “saturation models” for hadron production in AA collisions [26–28]. In the “hard GV” model at LHC energy, the remnants of Cronin effect at $p_T \sim 3$ GeV are overwhelmed by shadowing and the calculation in this region cannot be considered reliable as yet. The $R_M = 1.05$ at $p_T \simeq 40$ in Ref. [7] is a result of antishadowing in the EK98 parametrization and is not related to multiple initial state scatterings.

As discussed in the introduction, experimental reconstruction of minijets at ALICE should be possible in pA collisions for minijet transverse momenta $p_T \gtrsim 5$ GeV. The p_T -spectrum of the partons which will hadronize giving the observed minijet may be obtained by setting $D_i^h = \delta(z - 1)$ in Eqs. (1) and (6). This may be very interesting, because pQCD computations suffer from large uncertainties in

³Note however that the new parametrization, which predicts a much larger gluon shadowing at $x \lesssim 10^{-2}$ than the “old” one [12], seems ruled out by data on the ratio of Sn and Ca F_2 structure functions [34].

the determination of FF's at large z , where they are only loosely constrained by existing data [21]. For this reason I listed in Table 3 also the Cronin parameters for the case of parton production. However, jet reconstruction efficiency should be accurately evaluated to assess the usefulness of this observable.

Table 3 shows that there are large theoretical uncertainties in the extrapolation of the Cronin effect from lower energies to LHC energy. A major source of uncertainty for most of the models is the size of nuclear shadowing and anti-shadowing at small x , see Ref. [34] for a detailed discussion and comparison of the existing parametrizations. For example the HIJING parametrizations [12, 13] predict more gluon shadowing than the EKS98 [14] at small $x \lesssim 10^{-2}$. At LHC this is the dominant region at mid-rapidity and medium-small transverse momenta. On the other hands the HIJING parametrizations predict less antishadowing than EKS98 at $x \gtrsim 10^{-1}$, which is the dominant region at large enough p_T at all energies. At LHC all these effects may lead up to a factor 2 uncertainty in the height of the Cronin peak R_M .

In conclusion, a pA run at LHC is necessary both to test theoretical models for particle production in a cleaner experimental situation than in AA collisions, and to be able to make reliable extrapolations to AA collisions, which is the key to disentangle known effects and new physics. Since, as we have seen, the nuclear effects are potentially large, it would be even preferable to have a pA run at the same energy as the AA run. In addition, the A systematics, or the study of collision centrality cuts, would be interesting since would allow to change the opacity of the target – then the size of the Cronin effect – in a controllable way. Finally, let me remark that the η -systematics of the Cronin effect has been considered in the literature only in Ref. [6]. However, as discussed also in [33], given the large pseudorapidity coverage of CMS this observable might be a very powerful handle for the understanding of the effect. It would allow to systematically scan nuclear targets in the low- x region, and would help to test the proposed models, in which the rapidity affects the size of the Cronin effect in rather different ways.

ACKNOWLEDGEMENTS

I would like to thank M. Gyulassy, B. Kopeliovich, P. Lévai, D. Treleani, X. N. Wang, I. Vitev and F. Yuan for many helpful discussions. This work is partially funded by the European Commission IHP program under contract HPRN-CT-2000-00130.

References

- [1] CERN Yellow report on “Hard Probes in Heavy Ion Collisions at the LHC”, to appear.
- [2] J. W. Cronin, H. J. Frisch, M. J. Shochet, J. P. Boymond, R. Mermod, P. A. Piroué and R. L. Sumner, *Phys. Rev. D* **11** (1975) 3105.
- [3] X. N. Wang, *Phys. Rev. C* **61** (2000) 064910.
- [4] Y. Zhang, G. Fai, G. Papp, G. G. Barnafoldi and P. Levai, *Phys. Rev. C* **65** (2002) 034903.
- [5] B. Z. Kopeliovich, J. Nemchik, A. Schaefer and A. V. Tarasov, *Phys. Rev. Lett.* **88** (2002) 232303.
- [6] A. Accardi and D. Treleani, *Phys. Rev. D* **64** (2001) 116004.
- [7] I. Vitev and M. Gyulassy, *Phys. Rev. Lett.* **89** (2002) 25++2301; I. Vitev, *private communication*.
- [8] K. Adcox *et al.* [PHENIX Collaboration], *Phys. Rev. Lett.* **88** (2002) 022301; K. Reyers [WA98 collaboration], arXiv:nucl-ex/0202018.
- [9] P. Levai, G. Papp, G. Fai, M. Gyulassy, G. G. Barnafoldi, I. Vitev and Y. Zhang, *Nucl. Phys. A* **698** (2002) 631; I. Vitev, M. Gyulassy and P. Levai, arXiv:nucl-th/0204019.
- [10] J. Kuhn, *Phys. Rev. D* **13** (1976) 2948; A. Krzywicki, J. Engels, B. Petersson and U. Sukhatme, *Phys. Lett. B* **85** (1979) 407. M. Lev and B. Petersson, *Z. Phys.* **C21** (1983) 155.

- [11] M. Lev and B. Petersson, *Z. Phys. C* **21** (1983) 155.
- [12] X. N. Wang and M. Gyulassy, *Phys. Rev. D* **44** (1991) 3501; *Comput. Phys. Commun.* **83** (1994) 307.
- [13] S. Y. Li and X. N. Wang, *Phys. Lett. B* **527** (2002) 85
- [14] K. J. Eskola, V. J. Kolhinen and C. A. Salgado, *Eur. Phys. J. C* **9** (1999) 61.
- [15] M. B. Johnson *et al.*, *Phys. Rev. Lett.* **86** (2001) 4483, *Phys. Rev. C* **65** (2002) 025203.
- [16] K. Kastella, *Phys. Rev. D* **36** (1987) 2734.
- [17] X. N. Wang, *Phys. Rept.* **280** (1997) 287.
- [18] E. Wang and X. N. Wang, *Phys. Rev. C* **64** (2001) 034901
- [19] J. W. Qiu and G. Sterman, arXiv:hep-ph/0111002; R. J. Fries, arXiv:hep-ph/0201311.
- [20] M. A. Braun, E. G. Ferreira, C. Pajares, D. Treleani, arXiv:hep-ph/0207303
- [21] X. F. Zhang, G. Fai and P. Levai, , *Phys. Rev. Lett.* in press [arXiv:hep-ph/0205008].
- [22] D. Antreasyan *et al.*, *Phys. Rev. D* **19** (1979) 764; D. E. Jaffe *et al.*, *Phys. Rev. D* **40** (1989) 2777; P. B. Straub *et al.*, *Phys. Rev. Lett.* **68** (1992) 452.
- [23] B. Kopeliovich, *private communication*.
- [24] P. Levai, *private communication*.
- [25] X. N. Wang, *private communication*.
- [26] K. Eskola, K. Kajantie, P. V. Ruuskanen, K. Tuominen, *Nucl. Phys. B* **570** (2000) 379
- [27] D. Kharzeev and M. Nardi, *Phys. Lett. B* **507** (2001) 121.
- [28] A. Accardi, *Phys. Rev. C* **64** (2001) 064905.
- [29] E. Iancu, A. Leonidov and L. McLerran, arXiv:hep-ph/0202270.
- [30] K. J. Eskola, H. Honkanen, V. J. Kolhinen, J. W. Qiu and C. A. Salgado, arXiv:hep-ph/0211239, and contribution on nonlinear terms in DGLAP evolution in Ref. [1].
- [31] For a summary of recent results on non-Abelian energy loss see R. Baier, P. Levai, I. Vitev, U. Wiedemann, D. Schiff and B. G. Zakharov, in [1] and references therein.
- [32] K. J. Eskola and H. Honkanen, *Nucl. Phys. A* **713** (2003) 167.
- [33] I. Vitev, “Leading order pQCD hadron production and nuclear modification factors at RHIC and the LHC” in Ref. [1] [arXiv:hep-ph/0212109].
- [34] K. J. Eskola, H. Honkanen, V. J. Kolhinen and C. A. Salgado, *Phys. Lett. B* **532** (2002) 222; K. J. Eskola, H. Honkanen, V. J. Kolhinen, P. V. Ruuskanen and C. A. Salgado, “nPDF: process-independent features” in Ref. [1].